Pushing limits on generic squarks and gluinos with 13 TeV data

E. S. Kuwertz
on behalf of the ATLAS and CMS Collaborations
*Department of Physics and Astronomy, University of Victoria,
Victoria, British Columbia, Canada*

The Large Hadron Collider delivered pp collision data at a record energy of $\sqrt{s} = 13$ TeV during 2015 and 2016. This increase in centre-of-mass energy from 8 to 13 TeV yields a significant increase in the production cross section for squarks and gluinos. Here, the first results of dedicated searches for strongly produced supersymmetric particles making use of the full 13 TeV dataset from 2015 and 2016 are presented by the ATLAS and CMS Collaborations. No significant excess beyond the Standard Model expectation is observed in any analysis, and limits are placed on sparticle masses in the context of Supersymmetry-inspired simplified models.

1 Introduction

Supersymmetry [1,2,3,4,5,6] (SUSY) is a highly favoured extension to the Standard Model (SM), which postulates that for every particle in the SM there exists a supersymmetric partner particle. These supersymmetric particles (*sparticles*) differ from their SM counterparts by a half unit of spin, with the squarks ($\tilde{q}$) being the scalar partners to the SM quarks and gluinos ($\tilde{g}$) the fermionic partners to the SM gluons. Should these sparticles exist at the TeV scale, they could be accessible at the LHC collision energy, with a production rate such that they could be detected by the LHC experiments. In this case, SUSY could offer a solution to the hierarchy problem, and for R-Parity conserving (RPC) models the lightest supersymmetric particle (LSP) may present a candidate for Dark Matter.

A comprehensive search program was carried out by the ATLAS [7] and CMS [8] experiments during the LHC Run 1 (8 TeV), which failed to yield any significant evidence for beyond-Standard Model (BSM) physics. The higher collision energy in Run 2 (13 TeV) offers a large increase in the production cross section of squarks and gluinos, thus the first searches to take advantage of this new dataset are those with a focus on squark and gluino production. The searches presented herein make use of the 13 TeV dataset, with results from 36.1 fb^{-1} and 35.9 fb^{-1} of pp collision data from ATLAS and CMS, respectively.

Most of the analyses discussed in these proceedings consider R-Parity conserving SUSY models, and so target final states with high transverse momentum (high-p_{T}) objects and the large missing transverse momentum (E_{T}^{miss}) characteristic of weakly interacting LSPs escaping the detector. Examples of the SUSY signal topologies probed by such searches can be seen in Figure 1, with squarks or gluinos being pair-produced and subsequently undergoing either direct or cascade decays to the stable LSP. In other cases, where R-Parity violating (RPV) decays are considered, analyses select multi-object final states indicative of an unstable LSP decaying to multiple SM particles. Two examples of such signal models are illustrated in Figure 2.

Despite the wide range of final states and signal scenarios probed, the general analysis

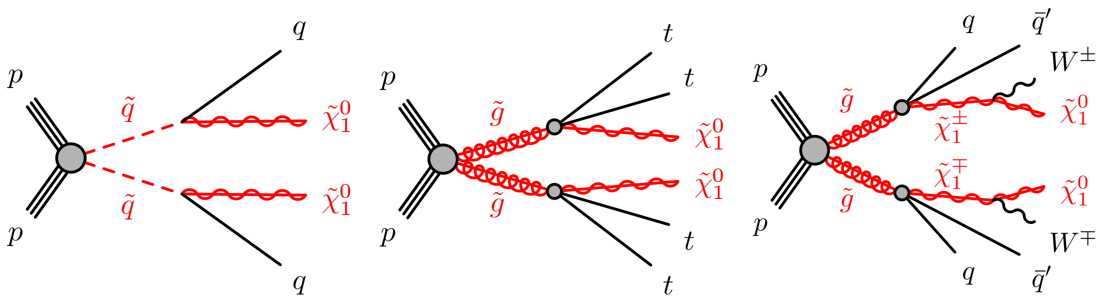

Figure 1 – Example decay topologies [11,13] for three simplified models considered by analyses targetting RPC scenarios. These models include direct squark (left) and gluino (middle, right) production, with subsequent direct decays via off-shell squarks (left, middle), or otherwise via intermediate bosons (right).

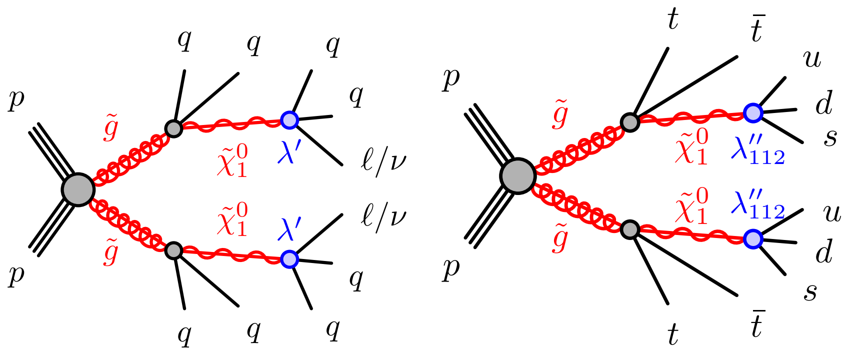

Figure 2 – Example decay topologies [16] for two simplified models considered by analyses targetting RPV scenarios. These models include direct gluino production, with subsequent decays via top squarks (left) or light squarks (right), with LSP decays to $qq\ell/\nu$ (left) or uds (right).

strategy follows a similar structure for all analyses considered. Control regions, designed to be dominated by the background process of interest, are constructed to measure the reducible backgrounds. Monte Carlo (MC) samples modelling the relevant background process are normalised to data in these regions, with this global scale factor being applied to the same process in the signal regions (SR). Irreducible backgrounds are often final state specific, and data-driven estimates are commonly exploited in order to model these processes in the SRs. The background estimations are cross-checked either in dedicated validation regions (VRs), or else by way of MC or data closure tests.

2 All hadronic searches

The first class of searches discussed here are those that consider final states with jets and missing transverse momentum. These analyses seek to exploit the large branching fractions of squarks and gluinos to jets. With large E_{T}^{miss} and high-p_{T} jets expected in the case of high gluino/squark masses and heavy or potentially boosted LSPs, simple variables such as H_{T} (where H_{T} is the scalar sum of the p_{T} of the jets in the event) and E_{T}^{miss} can be used to effectively isolate signal-like events. The H_{T}-H_{T}^{miss} analysis [9] (where H_{T}^{miss} is defined as the negative vector sum of the p_{T} of the jets in a given event) from CMS employs just such a strategy. In order to cover as much kinematic phase-space as possible, the analysis divides the H_{T}-H_{T}^{miss} plane into 10 exclusive regions, with those themselves being further split into 5 (4) bins in (b-tagged) jet multiplicity, resulting in a total of 174 search regions. Other analyses make use of more involved techniques. For example, the M_{T2} CMS analysis [10], while also making use of jet multiplicity, b-jet multiplicity and H_{T}, has SRs with exclusive bins in $M_{\mathrm{T2}} =$

$\min_{\vec{p}_{\mathrm{T}}^{\mathrm{missX(1)}}+\vec{p}_{\mathrm{T}}^{\mathrm{missX(2)}}=\vec{p}_{\mathrm{T}}^{\mathrm{miss}}} [\max(M_{\mathrm{T}}^{(1)}, M_{\mathrm{T}}^{(2)})]$, where the final state objects are clustered to form two pseudo-jets and $M_{\mathrm{T}}^{(i)}$ is the M_{T} of pseudo-jet $J(i)$ paired with one of the trial vectors $\vec{p}_{\mathrm{T}}^{\mathrm{miss}X(i)}$: $(M_{\mathrm{T}}^{(i)})^2 = (m_{J(i)})^2 + m_X^2 + 2(E_{\mathrm{T}}^{J(i)} E_{\mathrm{T}}^{X(i)} - \vec{p}_{\mathrm{T}}^{J(i)} \cdot \vec{p}_{\mathrm{T}}^{X(i)})$.

The SM multijet background tends to be largely confined to low M_{T2}, making this a powerful discriminant for searches that probe all hadronic final states. Other analyses enforce $\Delta\phi$ cuts between the final state jets and the E_{T}^{miss} in order to reject events in which fake E_{T}^{miss} is introduced via mismeasurement of final state objects. This approach is adopted by the ATLAS zero lepton analysis [11], which uses two distinct, complementary techniques to isolate signal-like events. The m_{eff}-based part of the analysis enforces high m_{eff} thresholds in the SRs, where $m_{\mathrm{eff}} = \sum_{i=1}^{n} |\vec{p}_{\mathrm{T}}^{(i)}| + E_{\mathrm{T}}^{miss}$, in order to target models with high mass squarks or gluinos. In addition, regions requiring $\geq 2-5$ jets are constructed to target events where gluinos or squarks undergo direct decays, whereas SRs with higher jet multiplicity requirements ($\geq 5-6$ jets) aim to isolate scenarios with longer decay chains, such as those illustrated in Figure 1 (middle). Finally, dedicated SRs that use large-radius jets probe models where the mass difference between the produced heavy sparticle and the LSP is large enough that intermediate bosons are highly boosted. These techniques are complemented by further SRs defined using the so-called *recursive jigsaw reconstruction technique* [12]. For topologies such as those in Figure 1 (left), the recursive jigsaw variables allow enhanced sensitivity to compressed regions of kinematic phase space, where the squark and LSP masses are very close together.

With the multijet backgrounds being suppressed, the dominant backgrounds in the SRs of these searches originate from SM W+jets and $\mathrm{t\bar{t}}$. The W+jets and $\mathrm{t\bar{t}}$ backgrounds tend to enter the all hadronic SRs by way of a lepton from a W-decay being missed in the physics object reconstruction (so-called "lost-lepton" background), or else as a result of a hadronically decaying τ-lepton (so-called "hadronic τ" background). To model these backgrounds data control samples requiring a single isolated and well-identified lepton (electron or muon) are constructed. For the former case, the CMS analyses reweight the data samples according to the probability for one of the leptons to be missed. For the latter, data events containing isolated muons only are selected, and the muons are subsequently smeared according to the p_{T}-distribution expected from a hadronically decaying τ-lepton. Closure tests performed on MC background samples demonstrate the validity of the method, as illustrated in Figure 3.

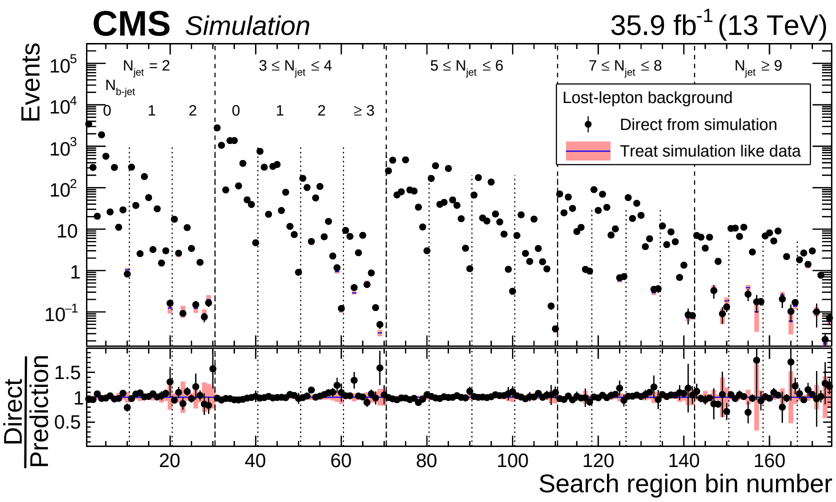

Figure 3 – Closure test showing the lost-lepton background determined directly from MC compared to the prediction from simulated electron and muon control samples [9].

The ATLAS analysis, while also making use of data control regions with isolated leptons, instead use these regions to normalise $\mathrm{t\bar{t}}$ and W+jets MC, enforcing orthogonality vetoing events containing b-tagged jets, respectively.

The observed data in all SRs are shown to be in agreement with the SM prediction. These results are interpreted in the context of several SUSY-inspired simplified models. In the case of the ATLAS searches, a combination of the recursive jigsaw and $m_{\rm eff}$ results is presented, deriving the limit at each mass point using the SR with the best-expected exclusion. The resulting exclusion contours from both the CMS $H_{\rm T}$-$H_{\rm T}^{miss}$ and ATLAS searches are presented in the $m(\tilde{q})-m(LSP)$ plane in Figure 4. These analyses exclude squark masses up to ~ 1.6 TeV and LSP masses up to ~ 850 GeV.

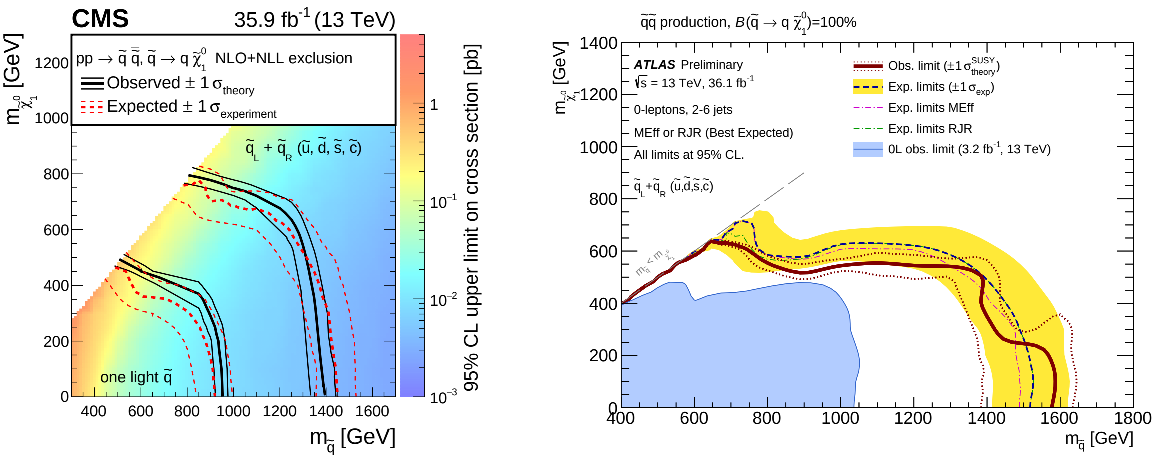

Figure 4 – Exclusion limits at 95 % confidence level for simplified models with direct squark production, where the squarks undergo direct decays to a quark and an LSP. The resulting exclusion countours are shown for the CMS $H_{\rm T}$-$H_{\rm T}^{miss}$ analysis [9] (left) and the ATLAS zero lepton analysis [11] (right).

3 Searches with leptons and jets

Several searches select events with leptons in the final state in order to essentially remove the SM multijet background from the SRs. The ATLAS 0/1-lepton ≥ 3 b-jets search [13] uses SRs with single isolated leptons in addition to those with a lepton veto so as to maximise sensitivity to simplified models with gluinos decaying via intermediate stops and sbottoms (the former being illustrated in the middle diagram of Figure 1). This analysis uses SRs with 5-7 (7-8) jets to target models with off-shell sbottoms (stops), with orthogonal SRs binned further in $m_{\rm eff}$. SRs with high $E_{\rm T}^{miss}$ and $m_{\rm eff}$ target high mass sparticle production, while SRs requiring a high-$p_{\rm T}$ leading jet probe models with small mass splittings. Control regions used to normalise the dominant backgrounds are also orthogonal, with cuts mimicking those of the SRs they model, and as such a simultaneous fit of all control and signal regions is possible in order to derive the limits for exclusion.

The CMS 1-lepton ≥ 6 jets analysis [14] also targets a simplified model with gluino mediated stops, and makes use of large-radius jets to target signal-like events containing boosted bosons. Here, 18 SRs, made orthogonal using cuts on (b-tagged) jet multiplicity, $E_{\rm T}^{miss}$, $M_{\rm J}(=\sum_{i\leq 4} m_{J,i})$ and $M_{\rm T}$, are used to derive limits on these models. The cuts on $M_{\rm T}$ ensure that the W+jets background in the SRs is negligible, resulting in a background composition dominated with SM top quark production. With the $M_{\rm J}$ distribution demonstrating invariance as a function of $M_{\rm T}$, the $M_{\rm J}$ distribution for this background is extrapolated from control regions with low $M_{\rm T}$.

The SRs of both the ATLAS 0/1-lepton ≥ 3 b-jets search and the CMS 1-lepton ≥ 6 jets search yield data in good agreement with the predicted SM background. Exclusion limits are presented in the $m(\tilde{g})-m(LSP)$ plane for models with intermediate stops in Figure 5. These analyses exclude gluino masses up to ~ 1.95 TeV and LSP masses up to ~ 1.2 TeV.

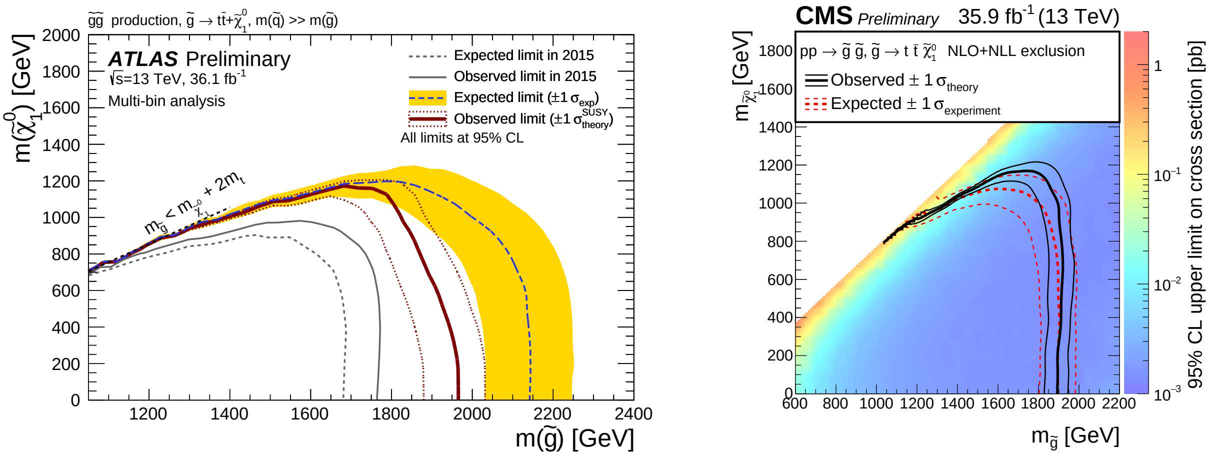

Figure 5 – Exclusion limits at 95 % confidence level for simplified models with gluino mediated stop production. The resulting exclusion countours are shown for the ATLAS 0/1-lepton ≥ 3 b-jets analysis [13] (left) and the CMS 1-lepton ≥ 6 jets analysis [14] (right).

The expected background from SM processes in the SRs are further reduced by selecting events containing two leptons with the same charge. This final state is probed by the CMS same sign (SS) 2-lepton analysis [15], which targets simplified models such as those illustrated in Figure 1 (middle and right). Events are separated into three categories according to lepton p_{T}. The first category requires both leptons to have low p_{T} (between 10 and 25 GeV), the second category requires the leading lepton to have $p_{\mathrm{T}}>$ 25 GeV and the sub-leading lepton to have $10 < p_{\mathrm{T}} <$ 25 GeV, and the third category requires both leptons in the event to have $p_{\mathrm{T}}>$ 25 GeV. Once divided into these three exclusive categories, events are further classified according to (b-tagged) jet multiplicity, E_{T}^{miss}, H_{T}, and M_{T}, resulting in 51 SRs in total. The main backgrounds in this analysis are estimated using data. The non-prompt lepton background makes use of a tight-to-loose lepton ratio based on data control samples, and the background due to charge mis-identification is modelled using a data sample containing events with two oppositely-charged leptons reweighted according to the charge-misidentification probability.

No significant excess is observed in any of the SRs in this analysis. The resulting exclusion limits in the $m(\tilde{g}) - m(LSP)$ plane for the simplified model with gluino decays via intermediate W-bosons are shown in Figure 6.

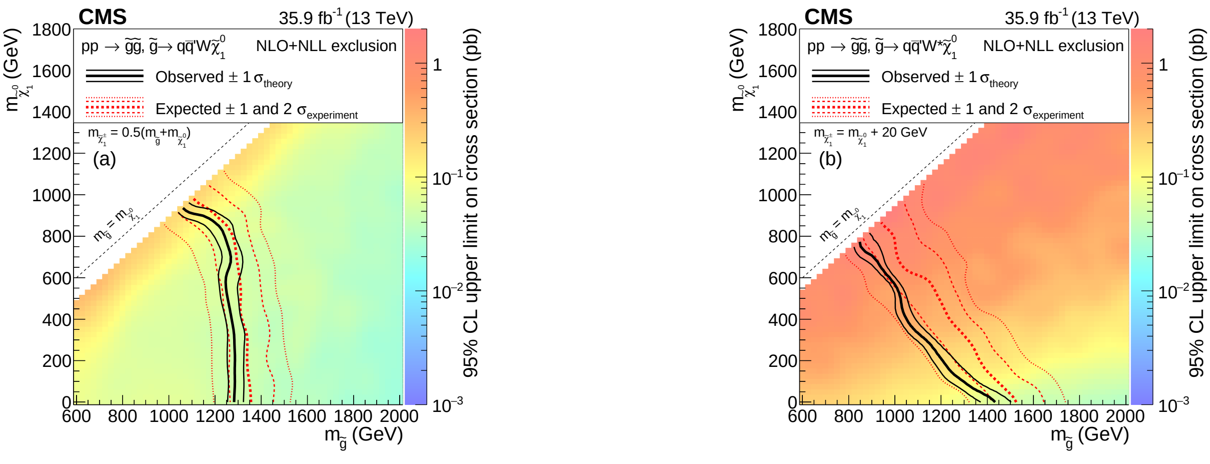

Figure 6 – Exclusion limits at 95 % confidence level [15] for simplified models with gluino production, with the gluinos following one-step decays via W-bosons. The resulting exclusion countours are shown assuming $m(\tilde{\chi}_1^{\pm}) = 0.5(m(\tilde{g}) + m(LSP))$ (left) and assuming $m(\tilde{\chi}_1^{\pm}) = m(LSP) + 20$ GeV (right).

Here the limits are presented with differing assumptions on the chargino mass. In one case the chargino mass is set halfway between the gluino and LSP mass, and the other case assumes a chargino mass only 20 GeV above the LSP mass. The results from the low-p_{T} lepton SRs are of particular importance to drive the exclusion for the latter case, where there is very little kinematic phase space between the chargino and LSP.

In order to target SUSY scenarios with RPV it is important to tailor the SR event selection accordingly. Here, requirements on large E_{T}^{miss} are less relevant, with the focus being rather on high object multiplicity final states. The ATLAS 1-lepton multijet analysis [16] aims to probe signal topologies such as those illustrated in Figure 2. Events are selected with ≥ 5 jets with $p_{\mathrm{T}}>$ $40, 60, 80$ GeV, and are then separated according to jet multiplicity. The highest jet multipicity SR accepts events with 12 jets. Those events with exactly $5, 6$ and 7 jets none of which are b-tagged, are further divided based on the charge of the leading lepton in the event, or whether or not they contain two same-flavour opposite-sign leptons within $81 < m_{\ell\ell} < 101$ GeV.

In order to extrapolate the dominant W+jets ($t\bar{t}$) in the b-veto ($\geq 1b$-tagged jet) regions, a scaling law is used. For $t\bar{t}$, the b-tagged jet distribution is taken from a sample of events with a 5 jet requirement. The evolution in jet multiplicity is then parameterised using the probability to get additional b-tags thereafter. A closure test, demonstrating the validity of the method, is performed using semi-leptonic and dileptonic $t\bar{t}$ MC, as well as a dileptonic $t\bar{t}$ enriched data sample, as shown in Figure 7. In all cases the data or simulation follow closely the parameterisation.

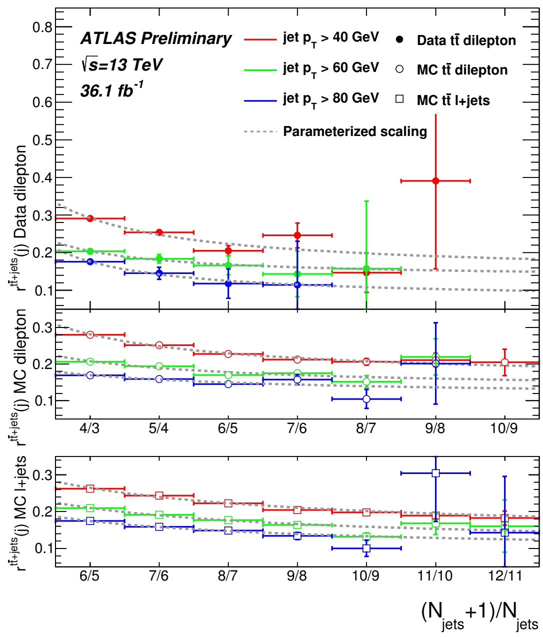

Figure 7 – Validation of the jet-scaling parameteristion used in the ATLAS 1-lepton multijet analysis [16]. The plot shows the $N_j/(N_j+1)$ event ratio in semi-leptonic, dileptonic $t\bar{t}$+jets events, with the ratio in data or simulation overlaid with a line indicated the relevant parameterisation.

The data in the SRs are in good agreement with the background prediction, and limits are derived on several simplified models with RPV couplings. Exclusion limits are shown for one of the models illustrated in Figure 8, with the best sensitivity coming from the SRs with an 80 GeV jet p_{T} requirement. For the model with gluino decays via virtual stops and LSP decays to uds, the analysis exclude gluino masses up to ~ 2 TeV and LSP masses up to ~ 1.4 TeV.

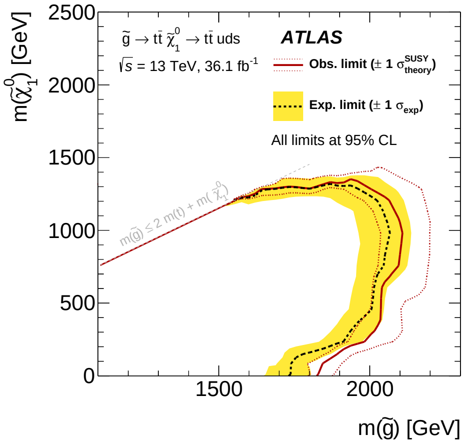

Figure 8 – Exclusion limits at 95 % confidence level from the ATLAS 1-lepton multijet analysis [16] for a simplified model with gluino production, with subsequent decays via top squarks, with LSP decays to *uds*.

4 Summary

The LHC had a productive year during 2016, providing a large 13 TeV dataset for experiments. The first SUSY searches to exploit this high centre-of-mass energy relative to 8 TeV were those targetting strongly produced squarks and gluinos. No significant excesses are reported in the analyses presented in this document, with the mass limits on squarks and gluinos being pushed ever further. New results are still expected for these production modes in different final states, with more results from SUSY searches dedicated to electroweak production on the way. There is still much to learn at 13 TeV, and the existing dataset is set to grow again when data-taking resumes in 2017.

References

1. Yu. A. Golfand and E. P. Likhtman, JTEP **13**, (1971) 323.
2. D. V. Volkov and V. P. Akulov, *Phys. Lett.* B **46**, (1973) 109.
3. J. Wess and B. Zumino, *Nucl. Phys.* B **70**, (1974) 39.
4. J. Wess and B. Zumino, *Nucl. Phys.* B **78**, (1974) 1.
5. S. Ferrara and B. Zumino, *Nucl. Phys.* B **79**, (1974) 413.
6. A. Salam and J. A. Strathdee, *Phys. Lett.* B **51**, (1974) 353.
7. ATLAS Collaboration, JINST **3**, (2008) S08003.
8. CMS Collaboration, JINST **3**, (2008) S08004.
9. CMS Collaboration, arXiv:1704.07781 [hep-ex].
10. CMS Collaboration, CMS-PAS-SUS-16-036, URL: http://cds.cern.ch/record/2256872.
11. ATLAS Collaboration, ATLAS-CONF-2017-022, URL: http://cds.cern.ch/record/2258145.
12. P. Jackson, C. Rogan and M. Santoni, *Phys. Rev.* D **95**, (2017) 3.
13. ATLAS Collaboration, ATLAS-CONF-2017-021, URL: http://cds.cern.ch/record/2258143.
14. CMS Collaboration, CMS-PAS-SUS-16-037, URL: http://cds.cern.ch/record/2256652.
15. CMS Collaboration, arXiv:1704.07323 [hep-ex].
16. ATLAS Collaboration, arXiv:1704.08493 [hep-ex].